Voltage-controlled entanglement and quantum-information transfer between spatially separated quantum-dot molecules

Xin-You Lü, Jing Wu, Li-Li Zheng, and Zhi-Ming Zhan

Phys. Rev. A **83**, 042302 — Published 4 April 2011

DOI: 10.1103/PhysRevA.83.042302

Voltage-controlled entanglement and quantum information transfer between spatially separated quantum dot molecules

Xin-You Lü[1],* Jing Wu[2], Li-Li Zheng[1], and Zhi-Ming Zhan[3]

[1]*School of Physics, Ludong University, Yantai 264025, P. R. China*

[2]*Institute of Advanced Nanophotonics State Key Lab of Modern Optical Instrumentation, Zhejiang University, Hangzhou 310027, P. R. China*

[3]*School of Physics and Information Engineering, Jianghan University, Wuhan 430056, P. R. China*

Abstract

We propose two schemes for generating entanglement and quantum state transfer (QST) between two spatially separated semiconductor quantum dot molecules (QDMs) based on the voltage-controlled tunneling effects. In the present schemes, two QDMs are trapped into two spatially separated cavities connected by a fiber, respectively. By numerically simulating the evolution of system, we show that the generation of entanglement and QST can be controlled by an external gate voltage in our schemes. Moreover, proposed schemes are robust against noise of system parameters.

PACS numbers: 03.67.Mn; 42.50.Dv; 78.67.Hc

*Electronic address: xinyou_lv@163.com

I. INTRODUCTION

Nowadays quantum-information theory has undergone a rapid development due to its attractive capabilities compared with classical-information theory. For example, quantum communication holds promise for secure transmission of secret messages and the faithful transfer of unknown quantum states. Quantum computers could dramatically speed up the solution of certain mathematical problems [1–3]. These quantum information processes always require generation of entanglement and implementation of quantum state transfer (QST) [4–10]. In recent years, a large number of theoretical and experimental schemes have been proposed for generating entanglement [11–27] and QST [28–35] in various quantum systems. For example, Eibl *et al.* [11] proposed a scheme for realizing the three-photon polarization-entangled state based on the spontaneous parametric down-conversion process. The four-particle entangled state of atoms has also been realized based on the measurement of photons [13]. Moreover, Cirac *et al.* [32] proposed a scheme for realizing the QST process between two distant atoms within the framework of cavity quantum electrodynamics (CQED). Most of them, however, require the use of atomic gas, which cannot be conveniently used in devices that have good scalability, such as those based on solid state system.

Recently, it has been shown that the semiconductor quantum dots (SQDs) have properties similar to those of atomic gas such as discrete energy levels and controllable coherent quantum evolution. With unique advantages, such as high nonlinear optical susceptibility, large electric-dipole moments of intersubband transitions, and great flexibility in designing devices [36–38], SQD system has wide applications in the fields of quantum optics and quantum information [39–48]. For example, the electromagnetically induced transparency (EIT) and the propagation of slow light have been realized in the SQD medium [43]. Villas-Bôas *et al.* [44] demonstrated the coherent control of tunnelling in a SQD molecule. Li *et al.* [47] proposed a scheme for realizing the all-optical quantum gate in a SQD system. Moveover, several interesting phenomena have been recognized when the SQD structure contains one or two electrons, such as controlled transfer of electrons between two SQDs [49, 50] and entanglement in two-electron SQD systems [51, 52], and so on. SQD therefore offers a feasible platform for realization of many quantum-information processes.

On the other hand, it has been shown that entanglement and QST between spatially separated quantum nodes is very useful for distributed quantum computation [53] and quantum

network [54, 55]. In recent years, a large number of schemes have been proposed for generating entanglement and QST between spatially separated atoms, which are individually trapped into distant optical cavities connected by fibers (i.e., cavity-fiber-cavity system) [56–61]. In particular, Ye *et al.* [58] proposed a scheme for deterministically generated entangled state of two spatially separated atoms in a coupled cavity-fiber-cavity system. Subsequently, Zhou *et al.* proposed a scheme for realizing the QST process between two spatially separated atoms [61]. In this paper, we propose two schemes for realizing the entanglement and QST between spatially separated QDMs in a cavity-fiber-cavity system. The major advantages of proposed schemes are as follows. (i) The QDM medium studied here has widely adjustable parameters. For example, the transition energies and dipole moments of QDMs can be manipulated well by accurately tailoring their shapes and sizes [36–38]. However, such property can hardly be found in the atomic medium. (ii) The tunneling rate of electron between two conduction-band levels can be effectively controlled by an external bias voltage, which further controlls the generation of entanglement and QST. (iii) Our schemes are robust with respect to system parameters, such as the frequency detuning Δ and cavity-fiber coupling constant η.

The remainder of this paper is organized into four parts as follows. In section II, we describe the model under consideration and derive the Hamiltonian of system. In section III, we discuss the generation of entanglement and QST between spatially separated QDMs from qualitative and quantitative aspects. In section IV, we analyze the influence of spontaneous decay of system on the generation of entanglement and QST. Finally, we conclude with a brief summary in section V.

II. MODEL AND HAMILTONIAN

As shown in Fig. 1(a), we consider a cavity-fiber-cavity system, which consists of two distant cavities (cavities A and B) connected by a fiber. Two homogeneous QDMs are trapped into the cavities A and B, respectively. The band structure of QDMs are shown in Fig. 1(b). The present QDMs consist of two SQDs [the left one (LD) and the right one (RD)] with different band structures coupled by tunnelling. At nanoscale interdot separation, the hole states are localized in the SQD and the electron states are rather delocalized. With the effective coupling of single-mode cavity, an electron is excited from the valence band to

the conduction band of LD. This electron can be transferred by the tunneling to RD. Here, it should be pointed out that the tunnel barrier in a QDM can be controlled by placing a gate electrode between the two SQDs. In the absence of the gate voltage, the conduction-band electron levels are out of resonance and the electron tunneling between two SQDs is very weak. Contrarily, in the presence of a gate voltage the conduction-band electron levels come close to resonance and the electron tunneling between the two SQDs is significantly enhanced. In addition, in the latter case the valence-band energy levels become more off-resonant and thus the hole tunneling can be neglected. Fig. 1(c) describes energy-level diagram of the QDMs. The ground state $|0\rangle_i$ $(i = A, B)$ has no excitations, the exciton state $|2\rangle_i$ has a pair of electron and hole in the LD, and the indirect exciton state $|1\rangle_i$ has one hole in the LD and one electron in the RD [45].

Then, under the dipole and rotating wave approximation, the interaction Hamiltonian of the QDM-cavity system can be written in the interaction picture as ($\hbar = 1$) [62–66]

$$H_I^{cq} = \sum_{i=A,B} \left[\Delta_i |2\rangle_i\langle 2| + \left(\Delta_i - \omega_{21}^i\right)|1\rangle_i\langle 1| + (g_i a_i |2\rangle_i\langle 0| + T_{ei}|2\rangle_i\langle 1| + h.c.)\right] \tag{1}$$

where the symbol $h.c.$ means Hermitian conjugate; $a_i^\dagger$ and a_i are the creation and annihilation operators for photons associating with the corresponding cavity modes. g_i is the coupling constant between QDM and cavity field. $\Delta_i = \omega_{20}^i - \nu_i$ denotes the frequency detuning, and $\omega_{ij} = \omega_i - \omega_j$. T_e is the tunneling coupling constant depicted on Fig. 1(b).

On the other hand, the interaction Hamiltonian of cavity-fiber can be written as

$$H_I^{cf} \;=\; \sum_{k=1}^{\infty} \left\{ \eta_{ik} b_k \left[a_A^\dagger + (-1)^k e^{i\phi} a_B^\dagger \right] + h.c. \right\}, \tag{2}$$

where b_k and $b_k^\dagger$ are the annihilation and creation operators for photons associating with fiber; η_k is the corresponding cavity-fiber coupling constant. Then, in the short fiber limit $(2L\bar{\nu})/(2\pi c) \ll 1$, where L is the length of fiber and $\bar{\nu}$ is the decay rate of the cavity field into a continuum of fiber modes, only the resonant mode of the fiber will interact with the cavity modes. For this case, the interaction Hamiltonian of cavity-fiber can be written as [53]

$$H_I^{cf} \;=\; \left[\eta b \left(a_A^\dagger + a_B^\dagger \right) + h.c. \right], \tag{3}$$

where b is the resonant mode of fiber, and the phase $(-1)^k e^{i\phi}$ in Eq. (2) has been absorbed

into the annihilation and creation operators of the modes of the second cavity field [57]. In addition, we also have set $\eta_A = \eta_B = \eta$ for simplicity in the above Hamiltonian.

Then, in the interaction picture, the total Hamiltonian of this cavity-fiber-cavity system is given by

$$\begin{aligned} H_I &= H_I^{cq} + H_I^{cf} \\ &= \sum_{i=A,B} \Big\{ \Delta_i |2\rangle_i\langle 2| + (\Delta_i - \omega_{21}^i)|1\rangle_i\langle 1| + \Big[g_i a_i |2\rangle_i\langle 0| + T_{ei}|2\rangle_i\langle 1| + \eta b(a_A^\dagger + a_B^\dagger) + h.c. \Big] \Big\} \end{aligned} \tag{4}$$

III. THE GENERATION OF ENTANGLEMENT AND QST

In this section, we begin to discuss the generation of entanglement (*scheme I*) and QST (*scheme II*) between spatially separated QDMs. First, let us qualitatively describe the processes of generating entanglement and QST based on *schemes I* and *II*, respectively.

Scheme I. For realizing the bipartite entangled state $|\Psi_e\rangle$ ($|\Psi_e\rangle = \frac{1}{\sqrt{2}}[|1\rangle_A|0\rangle_B + |0\rangle_A|1\rangle_B]$), we consider that the QDM A is initially in the state $|1\rangle_A$, the QDM B in the state $|0\rangle_B$, and all the field modes in vacuum state $|00\rangle_c|0\rangle_f$. Dominated by Hamiltonian (4), the evolution process of system can be generalized as follows. First of all, the electron in the QDM A will be transferred by tunnelling to LD from RD due to the present of gate voltage. Then, the electron will go back to valence-band of LD and emit a photon into the cavity A due to the interaction between QDM and cavity mode. The above two processes correspond to the transition $|1\rangle_A \xrightarrow{T_e} |2\rangle_A \xrightarrow{a_A^\dagger} |0\rangle_A$. Subsequently, the emitted photon will enter into cavity B though the fiber, and then the QDM B will absorb this photon and go though the transition $|0\rangle_B \xrightarrow{a_B} |2\rangle_B \xrightarrow{T_e} |1\rangle_B$ due to the corresponding tunnelling effects. Summing up the above description, it can be noticed that there is a nonlocal relation between two QDMs. When the QDM A is in the state $|1\rangle_A$, the QDM B will be in the state $|0\rangle_B$ or vice versa. So, along with the evolution of system, there should be an entangled state of QMDs $|\Psi_e\rangle = \frac{1}{\sqrt{2}}[|1\rangle_A|0\rangle_B + |0\rangle_A|1\rangle_B]$ at appropriate time.

Scheme II. In order to realize the QST process from the initial state $|\Psi\rangle_I = (\alpha|0\rangle_A + \beta|1\rangle_A) \otimes |0\rangle_B$ to the final state $|\Psi\rangle_F = |0\rangle_A \otimes (\alpha|0\rangle_B + \beta|1\rangle_B)$, we consider that the QDM A is initially in the superposition state $\alpha|0\rangle_A + \beta|1\rangle_A$, the QDM B in the state $|0\rangle_B$, and all the field modes in vacuum state $|00\rangle_c|0\rangle_f$. On the one hand, the evolution of system

will be the same with *scheme I*, when the QDM A is in the state $|1\rangle_A$ at the initial time. In this situation, the initial state $|1\rangle_A|0\rangle_B$ will evolve into state $|0\rangle_A|1\rangle_B$ at the end of a period of evolution. On the other hand, when QDM A is initially in the state $|0\rangle_A$, the state $|0\rangle_A|0\rangle_B$ will remain unchanged along with the evolvement of time. Summing up the above description, it can be noticed that the state of QDMs can evolve into the state $|0\rangle_A \otimes (\alpha|0\rangle_B + \beta|1\rangle_B)$ from the initial state $(\alpha|0\rangle_A + \beta|1\rangle_A) \otimes |0\rangle_B$ at appropriate time. In other words, the QST process between QDMs A and B can be realized based on our scheme.

Here, it can be generalized from the above discussion that the key for generation of entanglement and QST is the effects of electron tunnelling in the present QDMs. This tunnelling effects can be controlled by a external gate voltage applied to the QDM. If the gate voltage is very small (or zero), the conduction-band electron levels in the LD and RD will be out of resonance and the electron tunneling between two QDs can be neglected (i.e., $T_e = 0$). Such property can be used to control the generation of entanglement and QST in our schemes.

Until now, we have qualitatively discussed the feasibilities of realizing entanglement and QST in the present cavity-fiber-cavity system. Then, we will demonstrate quantitatively the generation of entanglement and QST based on our schemes. At the initial time, the state of system is considered to be in the state $|\psi(0)\rangle_E = |1\rangle_A|0\rangle_B|00\rangle_c|0\rangle_f$ for *scheme I* and the superposition state $|\psi(0)\rangle_{QST} = (\alpha|0\rangle_A + \beta|1\rangle_A) \otimes |0\rangle_B|00\rangle_c|0\rangle_f$ for *scheme II*. When $|\psi(0)\rangle_{QST} = \alpha|0\rangle_A|0\rangle_B|00\rangle_c|0\rangle_f$, the system state will remain unchanged along with the evolvement of time. On the other hand, when $|\psi(0)\rangle_E = |1\rangle_A|0\rangle_B|00\rangle_c|0\rangle_f$ (corresponding to *scheme I*) and $|\psi(0)\rangle_{QST} = \beta|1\rangle_A|0\rangle_B|00\rangle_c|0\rangle_f$ (corresponding to *scheme II*), the system state will evolve in the domination of the Schrödinger equation ($\hbar = 1$),

$$i\frac{\partial}{\partial t}|\psi(t)\rangle = H_I|\psi(t)\rangle, \tag{5}$$

where H_I is given by the Hamiltonian (4), and $|\psi(t)\rangle$ denotes the state of system at time t.

$|\psi(t)\rangle$ is restricted to the subspaces spanned by the following basis vectors

$$|\phi_1\rangle = |1\rangle_A|0\rangle_B|00\rangle_c|0\rangle_f, \tag{6a}$$

$$|\phi_2\rangle = |2\rangle_A|0\rangle_B|00\rangle_c|0\rangle_f, \tag{6b}$$

$$|\phi_3\rangle = |0\rangle_A|0\rangle_B|10\rangle_c|0\rangle_f, \tag{6c}$$

$$|\phi_4\rangle = |0\rangle_A|0\rangle_B|00\rangle_c|1\rangle_f, \tag{6d}$$

$$|\phi_5\rangle = |0\rangle_A|0\rangle_B|01\rangle_c|0\rangle_f, \tag{6e}$$

$$|\phi_6\rangle = |0\rangle_A|2\rangle_B|00\rangle_c|0\rangle_f, \tag{6f}$$

$$|\phi_7\rangle = |0\rangle_A|1\rangle_B|00\rangle_c|0\rangle_f, \tag{6g}$$

where n_{cA}, n_{cB}, and n_f in $|n_{cA}n_{cB}\rangle_c|n_f\rangle_f$ denote the photon numbers in the cavities and fiber, respectively. Then, in the above subspace, we solve numerically the Schrödinger equation [Eq. (5)] and present the evolution of populations in corresponding system states, as shown in Fig. 2. Without loss of generality, in the following numerical calculations, the parameters used are scaled with γ. Fig. 2(a) shows a half-half population for the states $|\phi_1\rangle$, $|\phi_7\rangle$ and zero population for other states at appropriate interaction time (e.g., $\gamma t = 2.88$). This case corresponds to the generation of the entangled state $|\Psi_e\rangle = \frac{1}{\sqrt{2}}[|1\rangle_A|0\rangle_B + |0\rangle_A|1\rangle_B]$. Fig. 2(b) shows that all population is completely transferred to the state $|\phi_7\rangle$ from the initial state $|\phi_1\rangle$ without populating other states at appropriate interaction time (e.g., $\gamma t = 31.5$). This case corresponds to the generation of QST process from QDMs A to B ($|\psi\rangle_I \rightarrow |\psi\rangle_F$).

In order to further explicitly show the generation of entanglement and QST, we also plot the fidelities of realizing entanglement (F_e) and QST (F_s) in Fig. 3. The F_e and F_s are defined as $F_e = |_f\langle 0|_c\langle 00|\langle\Psi_e|\psi(t)\rangle|^2$ and $F_s = |_f\langle 0|_c\langle 00|\langle\Psi_F|\psi(t)\rangle|^2$, respectively. From Fig. 3, it is shown that the entanglement and QST between two QDMs can be deterministically generated at appropriate time, which is consistent with the conclusion derived in Fig. 2 and our qualitative discussion in the previous parts of this section. In addition, it also can be seen that the plots of F_e and F_s change smoothly as a function of the dimensionless time γt. This characteristic is useful for switching off the interaction between QDMs and fields in time and obtaining the steady entangled state and QST.

Summing up the discussion above, it is noticed that the entanglement and QST can be deterministically generated under the ideal conditions of parameter. However, the ideal conditions of parameter may not be satisfied exactly in practical situations. In order to

study the influences of parameter mismatches on the fidelities of realizing entangled state and QST process, we plot F_e and F_s against the proportional coefficients s_1, s_2, coupling constant η, and frequency detuning Δ in Figs. 4 and 5. The proportional coefficients s_1 and s_2 satisfy relationships $g_B = s_1 g_A$ and $T_{eA} = T_{eB} = s_2 g_A$, respectively. Here, it should be pointed out that κ_A and κ_B are the decay rates of cavity modes, and they have been added phenomenologically in the calculations of Figs. 4 and 5. It is clearly shown from Figs. 4 and 5 that the F_e and F_s are insensitive with respect to the fluctuations of parameters s_1, s_2, η and Δ. As a result, the entanglement and QST process between two spatially separated QDMs can still be realized with high fidelity even though the ideal conditions of parameter could not be satisfied accurately in practical situations.

IV. EFFECTS OF QDM'S SPONTANEOUS DECAY AND PHOTON LEAKAGE

In Sec. III, we have shown that the entanglement and QST between two QDMs can be realized based on our schemes under the condition of neglecting the decay of system. However, the decay of system actually plays an important role in producing entanglement and QST experimentally. In this section, we will study the influences of QDM's decay and photon leakage out of the cavities and fiber on the generation of entangled state $|\Phi_e\rangle$ and QST process $|\Psi\rangle_I \rightarrow |\Psi\rangle_F$. Using the density-matrix formalism, the master equation for the density matrix of whole system can be expressed as:

$$\begin{aligned}\dot{\rho} \;=\; & -i\left[H_I, \rho\right] - \frac{\gamma_f}{2}\left(b_n^{\dagger} b_n \rho - 2 b_n \rho b_n^{\dagger} + \rho b_n^{\dagger} b_n\right) \\ & - \sum_{i=A,B}\left[\sum_{j=1,2} \frac{\gamma_{iq}^{j0}}{2}\left(\sigma_{jj}^{i}\rho - 2\sigma_{0j}^{i}\rho\sigma_{j0}^{i} + \rho\sigma_{jj}^{i}\right) + \sum_{m,n=0,1,2} \Gamma_{iq}^{mn}\sigma_{mm}^{i}\rho\sigma_{nn}^{i}\right. \\ & \left. + \frac{\kappa_i}{2}\left(a_i^{\dagger} a_i \rho - 2 a_i \rho a_i^{\dagger} + \rho a_i^{\dagger} a_i\right)\right]. \end{aligned} \tag{7}$$

where γ_{iq}^{j0} $(j = 1, 2)$ and Γ_{iq}^{mn} $(m, n = 0, 1, 2; m \neq n)$ are population decay rate and dephasing decay rate of QDM [43], respectively. Usually, Γ_{iq}^{mn} is the dominant mechanism, which originates not only from electron-electron scattering and electron-phonon scattering but also from inhomogeneous broadening due to scattering on interface roughness. κ_i and γ_f denote the decay rates of cavity fields and fiber modes, respectively. $\sigma_{jj}^{i} = |j\rangle_i\langle j|$ is the usual Pauli matrix. Via solving numerically the Eq. (7) in the subspace spanned by basis vectors (6), we present the effects of the decay rates γ_q, κ and γ_f on the fidelities of generating entangled

state and QST (F_e and F_s), as shown in the Figs. 6 and 7. In the above calculation, we have also chosen $\gamma_{Aq}^{20} = \gamma_{Bq}^{20} = \gamma_q$, $\Gamma_{Aq}^{mn} = \Gamma_{Bq}^{mn} = \Gamma_q^{mn}$, $\Gamma_q^{mn} = \Gamma_q^{nm}$, $\kappa_A = \kappa_B = \kappa$ without loss of generality. It is shown from the Fig. 6 that the influences of decay rates κ, γ_q, and γ_f on the fidelities F_e and F_s are very little when $\kappa = \gamma_q = \gamma_f = \Gamma \leq 0.01\gamma$. Even when $\Gamma = 0.01\gamma$, F_e and F_s are still larger than 96%. In order to further explicitly show the influences of decay rates γ_q, κ, and γ_f on F_e and F_s, respectively, we also plot F_e and F_S as a function of γ_q, κ, and γ_f in Fig. 7. Comparing three subplots of Fig. 7, it can be noticed that the influences of the cavity field decay rate κ and fiber decay rate γ_f on F_e and F_s are much smaller than that of QDM's decay rate γ_q, and hence they can be neglected safely in our scheme. This numerical result can be qualitatively explained as follows. In the present schemes, we have chosen the strong coupling condition between cavity and fiber (i.e., $\eta = 10\gamma$), and hence the cavity mode a_i and fiber mode b are only virtually excited in the whole interaction process. Therefore, the effects of photon leakage out of the cavity and fiber are suppressed strongly in the present schemes.

Before ending this section, let us briefly discuss the experimental feasibility of our scheme. First, the QDM considered here can be obtained by a unique combination of molecule beam epitaxy and *in situ* atomic layer precise etching [67, 68]. Secondly, the strong coupling between quantum dot and cavity modes has been realized in the previous studies [69–71], which improves the experimental feasibility of our schemes. Lastly, it should be pointed out that some obstacles for connecting effectively normal optical cavity to fiber may still exist. Therefore, we pin our hope on the coupled fiber-microcavity (i.e., microtoroid or microdisk resonators) system [72] for realizing our schemes experimentally. (i) The microcavity system can satisfy the low dissipation condition of cavity modes, which is required for implementing our schemes. (ii) The coupling between QDM and microcavity can be realized via locating QDM near the microcavity surface [73, 74]. (iii) The ideal coupling between microcavity and fiber has been realized experimentally in recent years [75–78].

V. CONCLUSION

In conclusion, we have proposed two schemes for realizing entanglement and QST between two spatially separated QDMs, respectively. In the present schemes, the generation of

entanglement and QST can be control effectively by the external gate voltage. Through numerical simulation, we show that the present schemes are robust with respect to photon leakage out of cavity and fiber. We hope that our schemes are promising for realization of new types of solid-state quantum information device.

Acknowledgments

The research was supported in part by the Natural Science Foundation of China (Grants No. 11005057, No. 10904033, and No. 10975054), and by the Foundation from the Ministry of the National Education of China (Grant No. 200804870051). We would like to thank Professor Ying Wu for helpful discussion and his encouragement.

---

[1] M. A. Nielsen and I. L. Chuang, Quantum Computation and Quantum Information (Cambridge University Press, Cambridge, U.K., 2000)

[2] C. H. Bennett and D. P. DiVincenzo, Nature (London) **404**, 247 (2000).

[3] D. Bouwmeester, J. W. Pan, K. Mattle, M. Eibl, H. Weinfurter, and A. Zeilinger, Nature **390**, 575 (1997).

[4] A. K. Ekert, Phys. Rev. Lett. **67**, 661 (1991).

[5] A. Barenco, D. Deutsch, A. Ekert, and R. Jozsa, Phys. Rev. Lett. **74**, 4083 (1995).

[6] W.-X. Yang, Z.-M. Zhan, and J.-H. Li, Phys. Rev. A **72**, 062108(1-6) (2005).

[7] A. Karlsson and M. Bourennane, Phys. Rev. A **58**, 4394 (1998).

[8] S. B. Zheng, and G. C. Guo, Phys. Rev. Lett. **85** 2392 (2000).

[9] M. Hillery, V. Bužek, and A. Berthiaume, Phys. Rev. A **59**, 1829 (1999).

[10] N. Gisin and S. Massar, Phys. Rev. Lett. **79**, 2153 (1997).

[11] M. Eibl, N. Kiesel, M. Bourennane, C. Kurtsiefer, and H. Weinfurter, Phys. Rev. Lett. **92**, 077901(1-4) (2004).

[12] J.-W. Pan, D. Bouwmeester, M. Daniell, H. Weinfurter, and A. Zeilinger, Nature (London) **403**, 515 (2000).

[13] X. B. Zou, K. Pahlke, and W. Mathis, Phys. Rev. A **68**, 024302(1-4) (2003).

[14] Q. A. Turchette, C. S. Wood, B. E. King, C. J. Myatt, D. Leibfried, W. M. Itano, C. Monroe and D. J. Wineland, Phys. Rev. Lett. **81** 3631 (1998).

[15] Y. Wu, M. G. Payne, E. W. Hagley and L. Deng, Phys. Rev. A **69** 063803 (2004).

[16] G.-C. Guo and Y.-S. Zhang, Phys. Rev. A **65**, 054302(1-3) (2002).

[17] S. B. Zheng, G.C. Guo, Phys. Rev. A **73** 032329 (2006).

[18] L.F. Wei, Y. Liu, F. Nori, Phys. Rev. Lett. 96 246803 (2006).

[19] L. Zhou, Z.R. Gong, Y. Liu, C.P. Sun, F. Nori, Phys. Rev. Lett. **101** 100501 (2008).

[20] J.Q. You, J. S. Tsai, and F. Nori, Phys. Rev. Lett. **19** 197902 (2002).

[21] Y.-F. Xiao, X.-B. Zou, and G.-C. Guo, Phys. Rev. A **75**, 012310(1-5) (2007).

[22] X. L. Zhang, K. L. Gao,and M. Feng, Phys. Rev. A **75**, 034308(1-4) (2007).

[23] Z.-R. Lin, G.-P. Guo, T. Tu, F.-Y. Zhu, and G.-C. Guo, Phys. Rev. Lett. **101**, 230501(1-4) (2008).

[24] G.-X. Li, H. Tan, M. Macovei, Phys. Rev. A **76** 053827 (2004); G.-X. Li, S. Ke, and Z. Ficek, Phys. Rev. A **79**, 033827(1-9) (2009).

[25] X. M. Hu, J.H. Zou, Phys. Rev. A **78** 045801 (2008); X. Li, X. M. Hu, Phys. Rev. A **80** 023815 (2009).

[26] C. F. Roos, M. Riebe, H. Haffner, W. Hansel, J. Benhelm, G. P. T. Lancaster, C. Becher, F. Schmidt-Kaler, and R. Blatt, Science **304**, 1478 (2004).

[27] C. A. Sackett, D. Kielpinski, B. E. King, C. Langer, V. Meyer, C. J. Myatt, M. Rowe, Q. A. Turchette, W. M. Itano, and C. M. D. J. Wineland, Nature (London) **404**, 256 (2000).

[28] F. W. Strauch, C. J. Williams, Phys. Rev. B **78** 094516 (1-7) (2008).

[29] M. Christandl, N. Datta, A. Ekert, A. J. Landahl, Phys. Rev. Lett. **92** 187902 (1-4) (2004).

[30] D. Leibfried, B. Demarco et al., Nature **422** 412 (2003).

[31] F. Schmidt-Kaler, H. Häffer et al., Nature **422** 408 (2003).

[32] J. I. Cirac, P. Zoller, H. J. Kimble, H. Mabuchi, Phys. Rev. Lett. **78** 3221 (1997).

[33] C. P. Yang, S. Chu, S. Han, Phys. Rev. Lett. **92** 117902 (1-4) (2004).

[34] M. A. Sillanpää, J. I. Park, R. W. Simmonds, Nature **449** 438 (2007).

[35] T. Pellizzari, Phys. Rev. Lett. **79** 5242 (1997).

[36] A. Zrenner, E. Beham, S. Stufler, F. Findeis, M. Bichler, G. Abstreiter, Nature (London) **418** 612 (2002).

[37] T.H. Oosterkamp, T. Fujisawa, W.G. van der Wiel, K. Ishibashi, R.V. Hijman, S. Tarucha,

L.P. Kouwenhoven, Nature (London) **395** 873 (1998).

[38] J. Kim, S.L. Chuang, P.C. Ku, C.J. Chang-Hasnain, J. Phys.: Condens. Matter, **16** S3727 (2004).

[39] J.R. Guest, T.H. Stievater et al., Phys. Rev. B **65** 241310(R) (2002).

[40] E. Paspalakis, Phys. Rev. B **67**, 233306 (2003).

[41] E. Paspalakis, Z. Kis, E. Voutsinas and A. F. Terzis, Phys. Rev. B **69**, 155316 (2004).

[42] E. Paspalakis, A. Kalini and A. F. Terzis, Phys. Rev. B **73**, 073305 (2006); S. G. Kosionis, A. F. Terzis and E. Paspalakis, Phys. Rev. B **75**, 193305 (2007).

[43] C.J. Chang-Hasnain, P.C. Ku, J. Kim, S.L. Chuang, Proc. IEEE **91** 1884 (2003), and references therein.

[44] J.M. Villas-Bôas, A.O. Govorov, S.E. Ulloa, Phys. Rev. B **69** 125342 (1-4) (2004).

[45] C.H. Yuan, K.D. Zhu, Appl. Phys. Lett. **89** 052115 (1-3) (2006).

[46] P. Kaer Nielsen, H. Thyrrestrup, J. Mork, B. Tromborg, Opt. Express **15** 6396 (2007).

[47] X. Li, Y. Wu, D.G. Steel, D. Gammon, T.H. Stievater, D.S. Katzer, D. Park, C. Piermarocchi, L.J. Sham, Science **301** 809 (2003).

[48] S. Sangu, K. Kobayashi, A. Shojiguchi, M. Ohtsu, Phys. Rev. B **69** 115334 (1-13) (2004).

[49] L.A. Openov, Phys. Rev. B **60** 8798 (1999).

[50] A.V. Tsukanov, Phys. Rev. B **73** 085308 (1-9) (2006).

[51] J.-L. Zhu, W.Chu, Z. Dai, and D. Xu, Phys. Rev. B **72** 165346 (1-7) (2005).

[52] A. V. Tsukanov, Phys. Rev. A **72** 022344 (1-8) (2005).

[53] S. Mancini and S. Bose, Phys. Rev. A **70**, 022307(1-4) (2004).

[54] T. Pellizzari, Phys. Rev. Lett. **79**, 5242 (1997).

[55] H. J. Kimble, Nature **453** 1023 (2008).

[56] L.-B. Chen, M.-Y. Ye, G.-W. Lin, Q.-H. Du, and X.-M. Lin, Phys. Rev. A **76** 062304(1-7) (2007).

[57] P. Peng and F.-L. Li, Phys. Rev. A, **75**, 062320(1-7) (2007).

[58] S.-Y. Ye, Z.-R. Zhong,and S.-B. Zheng, Phys. Rev. A, **77**, 014303(1-4) (2008).

[59] X.-Y. Lü, J.-B. Liu, C.-L. Ding, and J.-H. Li, Phys. Rev. A, **78**, 032305(1-6) (2008); X.-Y. Lü, L.-G. Si, M. Wang, S.-Z. Zhang and X. Yang, J. Phys. B: At. Mol. Opt. Phys. **41**, 235502(1-6) (2008).

[60] Z. Yin and F.-L. Li, Phys. Rev. A **75**, 012324(1-11) (2007).

[61] Y. L. Zhou, Y. M. Wang, L. M. Liang, and C. Z. Li, Phys. Rev. A **79** 044304 (1-4) (2009).

[62] Y. Wu, L. Wen, and Y. Zhu, Opt. Lett. **28**, 631 (2003).

[63] Y. Wu and X. Yang, Opt. Lett. **28**, 1793 (2003).

[64] J. Li, R. Yu, L. Si, X.-Y. Lü, and X. Yang, J. Phys. B **42** 055509 (1-7) (2009).

[65] Y. Wu and X. Yang, Appl. Phys. Lett. **91**, 094104 (2007).

[66] Y. Wu and P. T. Leung, Phys. Rev. A **60**, 630 (1999).

[67] P. M. Petroff, A. Lorke and A. Imamoğlu, Phys. Today **54** 46-52 (2001).

[68] G. J. Beirne, C. Hermannstädter, L. Wang, A. Rastelli, O. G. Schmidt and P. Michler, Phys. Rev. Lett. **96** 137401 (1-4) (2006).

[69] J. P. Reithmaier, G. Sek, A. Löffler et al., Nature **432** 179 (2004).

[70] K. Hennessy, A. Badolato, M. Winger et al., Nature, **445** 896 (2007).

[71] E. Waks, D. Sridharan, and J. Vuckovic, Proc. of SPIE, **6710** 67100L(1-11) (2007).

[72] K. J. Vahala, Nature, **424** 839 (2003).

[73] D. W. Vernooy and H. J. Kimble, Phys. Rev. A **55** 1239 (1997).

[74] Y.-F. Xiao, Z.-F. Han, and G.-C. Guo, Phys. Rev. A **73** 052324 (1-6) (1997).

[75] B. Min, L. Yang, and K. Vahala, Appl. Phys. Lett. **87** 181109(1-3) (2005).

[76] M. Hossein-Zadeh, and K. Vahala, Optics Express **15** 166 (2007).

[77] P. E. Barclay, K. Srinivasan, O. Painter, B. Lev, and H. Mabuchi, Appl. Phys. Lett. **89**, 131108(1-3) (2006).

[78] P.-B. Li, Y. Gu, Q.-H. Gong, and G.-C. Guo, Phys. Rev. A **79**, 042339(1-4) (2009).

[79] S. M. Spillane, T. J. Kippenberg, O. J. Painter, and K. J. Vahala, Phys. Rev. Lett. **91**, 043902(1-4) (2003).

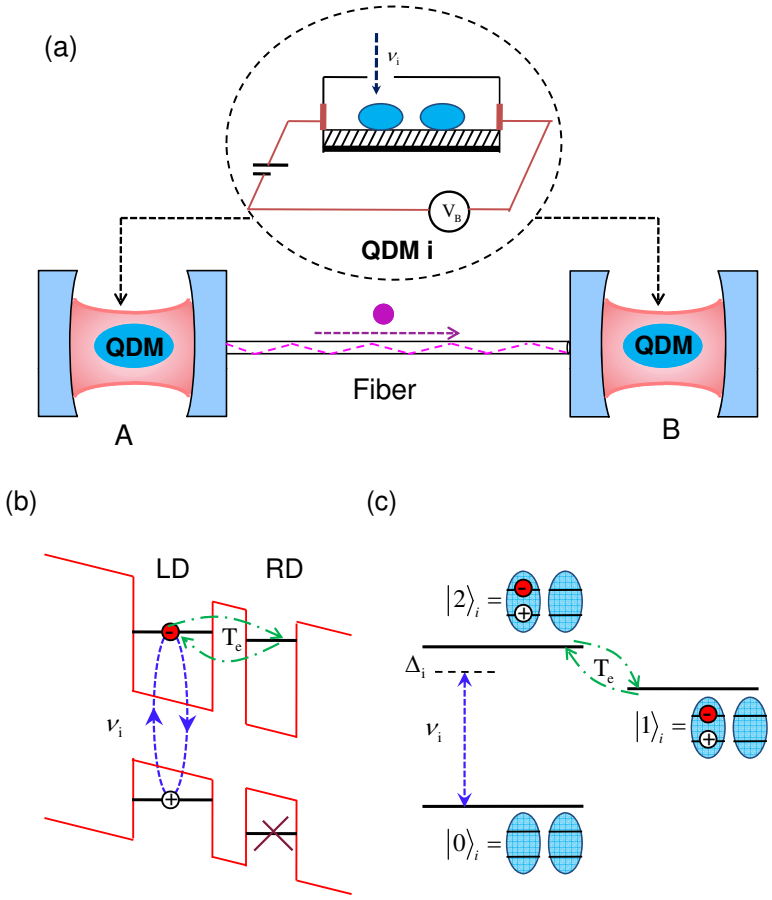

FIG. 1: (Color online) (a) The schematics of cavity-fiber-cavity system. Two coupled GaAs-AlGaAs asymmetrical QDMs are trapped into two cavities connected by a fiber, respectively. The schematic of the lateral geometry of QDM is presented. V_B is a bias voltage. (b) Band diagram of the QDM, which consists of two dots (the left dot (LD) and the right dot (RD)) with different band structures coupled by tunneling. With an external voltage applied to a gate electrode, the conduction-band levels get closer to resonance, and the coupling between conduction-band levels is greatly increased. Whereas the valence-band levels get more off-resonance, which results in effective decoupling of valence-band levels. (c) Schematic of the energy level arrangement under study. The cavity mode ν_i (i=A,B) induce one electron from the valence to the conduction-band in the LD, which can in turn tunnel to the RD. The ground state $|0\rangle_i$ (i=A,B) is the system without excitations, the direct exciton state $|2\rangle_i$ is a pair of electron and hole bound in the LD, and the indirect exciton state $|1\rangle_i$ is one hole in the LD with an electron in the RD. T_e denotes the electron-tunnelling intensity between two coupled QDs.

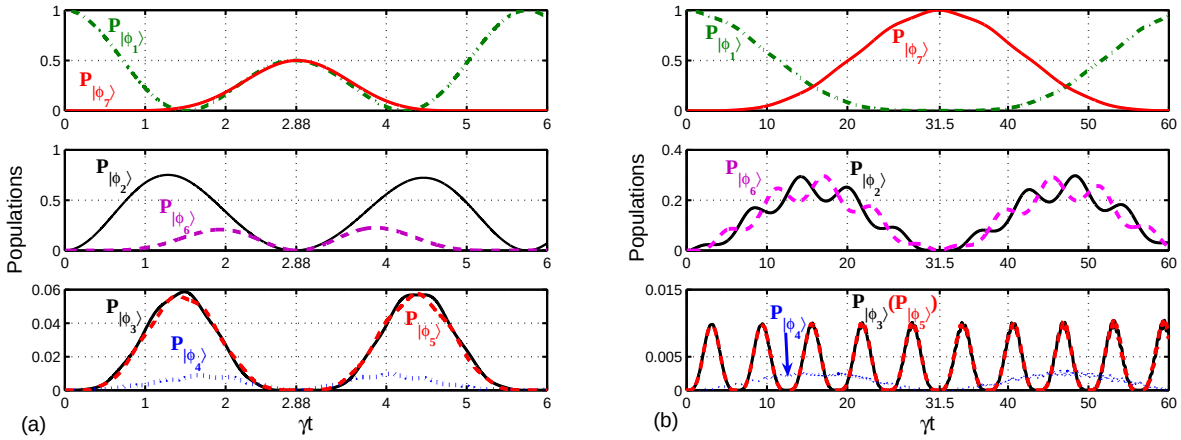

FIG. 2: (Color online) Time evolution of the populations corresponding to scheme I [panel (a)] and scheme II [panel (b)]. The parameters are scaled with γ and chosen as $g_A = \gamma$, $g_B = 2.43\gamma$, $T_{eA} = T_{eB} = 1.1\gamma$, $\omega_{21} = 0$ (resonant tunnelling), $\Delta = 0$, $\eta = 10\gamma$ for panel (a), and $g_A = g_B = \gamma$, $T_{eA} = T_{eB} = 0.1\gamma$, $\omega_{21} = 0$, $\Delta = 0$, $\eta = 10\gamma$, $\alpha = \sqrt{2}/\sqrt{3}$, $\beta = 1/\sqrt{3}$ for panel (b).

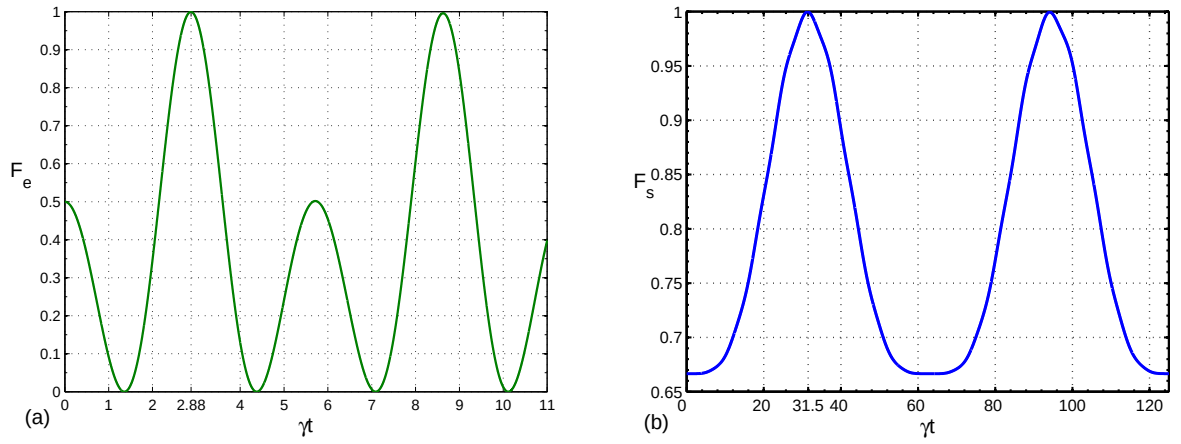

FIG. 3: (Color online) The fidelities of realizing entanglement [panel (a)] and QST [panel (b)] versus time γt. The parameters are same as Fig. 2.

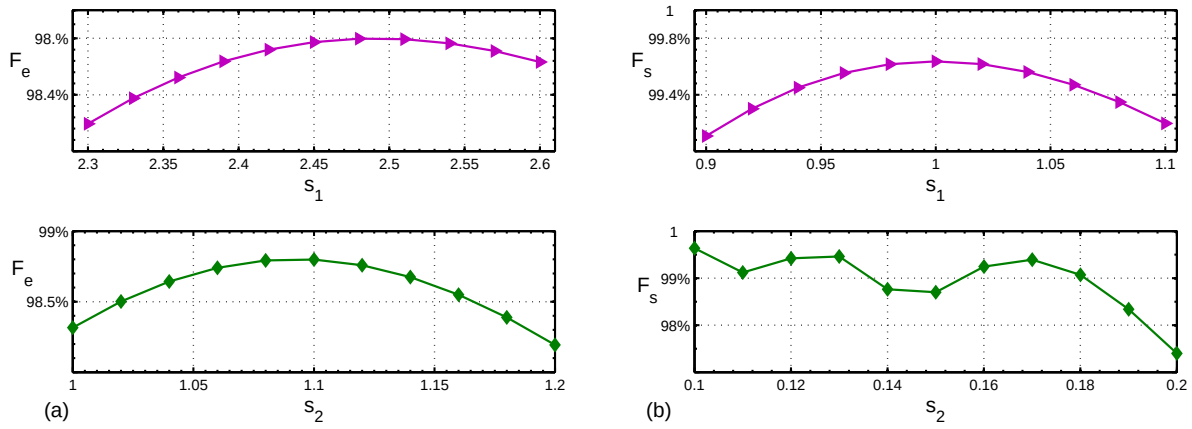

FIG. 4: (Color online) The fidelities of realizing entanglement [panel (a)] and QST [panel (b)] versus s_1 and s_2, respectively. The parameters are same as Fig. 2 except for the cavity decay rate $\kappa_A = \kappa_B = 0.1\gamma$.

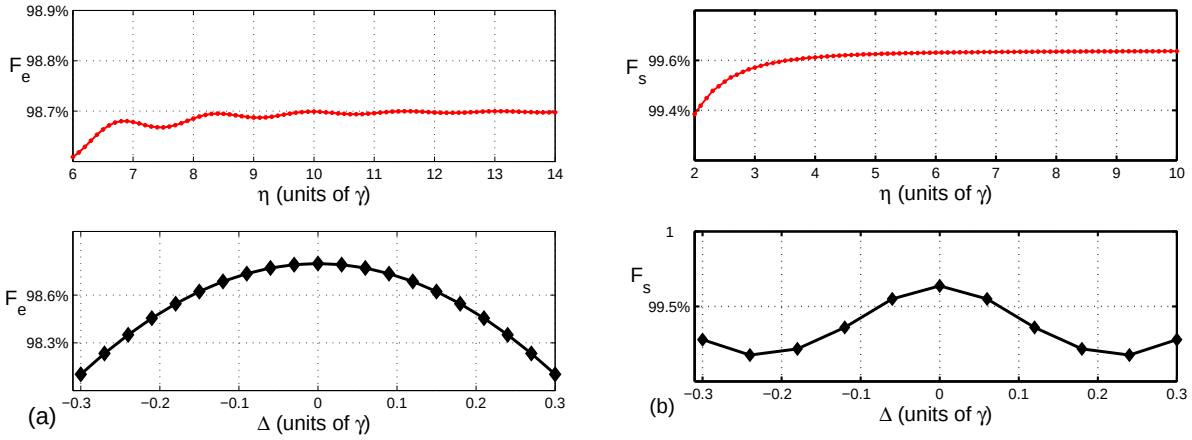

FIG. 5: (Color online) The fidelities of realizing entanglement [panel (a)] and QST [panel (b)] versus coupling constant η and frequency detuning Δ, respectively. The parameters are same as Fig. 2 except for the cavity decay rate $\kappa_A = \kappa_B = 0.1\gamma$.

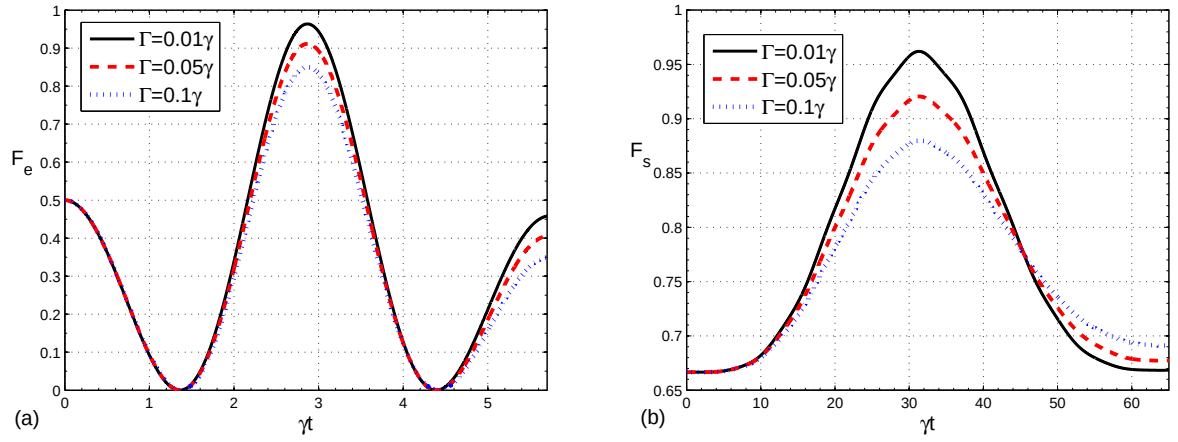

FIG. 6: (Color online)The fidelities of realizing entanglement [panel (a)] and QST [panel (b)] versus time γt for different decay rates Γ ($\gamma_q = \kappa = \gamma_f = \Gamma$). The parameters are same as Fig. 2 except for $\gamma_q^{10} = 0.001\gamma$, $\Gamma_q^{10} = 0.003\gamma$, $\Gamma_q^{20} = \Gamma_q^{21} = 0.03\gamma$.

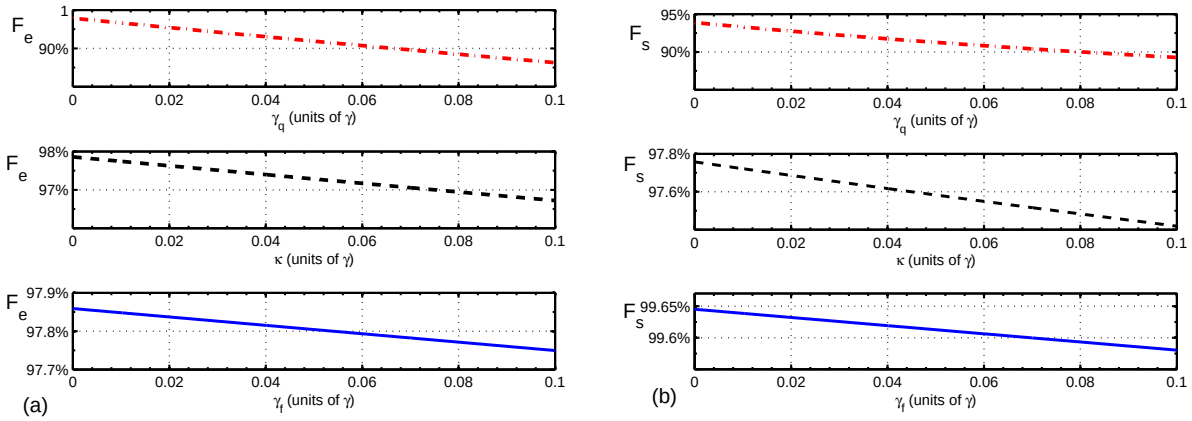

FIG. 7: (Color online) The fidelities of realizing entanglement [panel (a)] and QST [panel (b)] versus γ_q, κ, and γ_f, respectively. The system parameters are same as Fig. 6.